

JBMR SHORT REPORT***In vivo* UTE-MRI reveals positive effects of raloxifene on skeletal bound water in skeletally mature beagle dogs.**

Matthew R. Allen¹, Paul R. Territo², Chen Lin², Scott Persohn²,
Lei Jiang², Amanda A. Riley², Brian P. McCarthy²,
Christopher L. Newman¹, David B. Burr¹, and Gary D. Hutchins²

¹Department of Anatomy and Cell Biology, and ²Department of Radiology and Imaging Sciences, Indiana University School of Medicine, Indianapolis, IN, United States.

Keywords: hydration, cortical bone, SERMs, non-invasive imaging

Send Correspondence to:

Matthew R. Allen, PhD
Dept. of Anatomy and Cell Biology, MS 5035
Indiana University School of Medicine
635 Barnhill Dr.
Indianapolis, IN 46202
Tel: 317-274-1283
FAX: 317-278-2040
Email: matallen@iupui.edu

23 **ABSTRACT**

24 Raloxifene positively affects mechanical properties of the bone matrix in part through
25 modification of skeletal bound water. The goal of this study was to determine if raloxifene-
26 induced alterations in skeletal hydration could be measured *in vivo* using ultra-short echotime
27 magnetic resonance imaging (UTE-MRI). Twelve skeletally mature female beagle dogs
28 (n=6/group) were treated for 6 months with oral doses of saline vehicle (VEH, 1 ml/kg/day) or
29 raloxifene (RAL, 0.5 mg/kg/day). Following six months of treatment, all animals underwent *in*
30 *vivo* UTE-MRI of the proximal tibial cortical bone. UTE-MRI signal intensity versus echotime
31 curves were analyzed by fitting a double exponential to determine the short and long relaxation
32 times of water with the bone (dependent estimations of bound and free water, respectively).
33 Raloxifene-treated animals had significantly higher bound water (+14%; $p = 0.05$) and lower free
34 water (-20%) compared to vehicle-treated animals. These data provide the first evidence that
35 drug-induced changes in skeletal hydration can be non-invasively assessed using UTE-MRI.

36

37 INTRODUCTION

38 Raloxifene significantly reduces fracture risk despite minimal effects on bone mineral density⁽¹⁻
39 ³⁾. Preclinical studies in a dog model have documented a positive effect of raloxifene on
40 material-level biomechanical properties (the properties of the tissue independent of bone mass)
41 using both estimated material properties from whole bone tests (vertebra, femoral neck, rib) and
42 direct assessment on beams from femoral bone^(4,5). Recent work has identified changes in
43 skeletal hydration, specifically increases in matrix-bound water, as a key factor in this positive
44 material-level adaption of bone. Treatment with raloxifene for one year in beagle dogs led to
45 significantly more total skeletal water, assessed gravimetrically, and this was positively
46 associated with the bone's mechanical properties⁽⁶⁾. Ultra-short echotime MRI (UTE-MRI) can
47 differentiate hydration status of bone under various conditions⁽⁷⁻⁹⁾. More detailed assessment
48 of raloxifene's effects on bone hydration using UTE-MRI revealed that *ex vivo* soaking of cortical
49 bone (both dog and human) in raloxifene resulted in more matrix bound water compared to
50 control of bone⁽⁶⁾. As UTE-MRI may have potential for clinical application⁽¹⁰⁾, the goal of this
51 study was to test the hypothesis that UTE-MRI can be used *in vivo* as a diagnostic indicator to
52 detect changes in bone hydration caused by pharmacological interventions.

53 METHODS

54 *Experimental design*

55 Twelve skeletally mature female beagles (1-2 years old) were treated with one of two conditions
56 for 6 months (n=6 per group): daily oral saline vehicle (1 mL/kg) or daily oral raloxifene (0.5
57 mg/kg). Raloxifene was dissolved in 10% hydroxypropyl- β -cyclodextrin and administered at a
58 dose consistent with the clinical management of post-menopausal osteoporosis on a mg/kg
59 basis. This dose has been shown previously to alter mechanical properties in this animal model

1
2
3 60 following 6 months ⁽¹¹⁾ and one year of treatment ^(4,5,12). After six months of treatment, all
4
5 61 animals underwent *in vivo* UTE-MRI. All procedures were approved by the Indiana University
6
7 62 School of Medicine Animal Care and Use Committee, and were conducted in accordance with
8
9 63 NIH and USDA guidelines on animal care and use prior to the start of the study.
10
11

12 13 64 *Ultra-short Echotime MRI (UTE-MRI)* 14

15
16 65 Prior to imaging, anesthesia was induced with a combination of ketamine (8mg/kg) and
17
18 66 diazepam (0.3mg/kg) via the cephalic vein. Anesthesia was maintained on 1-2% Isoflurane
19
20 67 (balanced with medial grade oxygen) delivered at 2 L/min via mask. The hind limbs were
21
22 68 immobilized in a custom configured splint that permitted precise placement of the two channel
23
24 69 Miniflex[®] surface coils (Rapid MR International) laterally over the diaphysis inferior to the tibial
25
26 70 plateau. The splint and surface coils were then secured to a custom configured leg stabilization
27
28 71 platform permitting precise and repeatable iso-center alignment of the hindlimb and coils in the
29
30 72 scanner. Each animal was scanned on an Siemens 3T Tim Trio MRI using an 3D UTE
31
32 73 sequence with the following characteristics: TR (Time to repeat the sequence) 20 ms; TE1
33
34 74 (Echo time 1) variable (0.05, 0.06, 0.07, 0.08, 0.10, 0.12, 0.14, 0.20, 0.30, 0.40, 0.50, 0.60,
35
36 75 0.80, 1.0, 1.1 ms); TE2 (Echo time 2) 5 ms; Fat Saturation; Average 1, Excitation Flip Angle 50°;
37
38 76 Normalization Filter; Acquisition Matrix 80x80x80; Field of View 50x50; Spatial Resolution
39
40 77 0.63x0.63x0.63 mm, and TA (Total acquisition time) 28 min. Fat saturation was applied to
41
42 78 prevent signal oscillation with TE ⁽⁶⁾ and although this may slightly impact the measured bound
43
44 79 water fraction ⁽¹³⁾, we felt it was a reasonable compromise to avoid potentially greater error due
45
46 80 to signal oscillation.
47
48
49
50

51
52 81

53 54 82 *Image Analysis* 55 56 57 58 59 60

1
2
3 83 Image volumes for both variable (TE1) and fixed (TE2) echo times were imported, segmented,
4
5 84 and quantified using Analyze 11.0 (AnalyzeDirect). Marrow and cortical bone for each image
6
7 85 series per animal were segmented on the shortest TE1 image using a region growing technique,
8
9 86 where the distal and proximal limits were prescribed at a fixed distance from the center of the
10
11 87 FOV. Segmented regions were then extracted for all TE1 and TE2 images volumes, thereby
12
13 88 permitting secondary analysis of the UTE signal. To correct for receiver gain offset differences
14
15 89 between successive images, the following scaling was applied:
16
17
18

$$19 \quad F(TE1, j) = \frac{Max[M(TE2, j)]}{M(TE2, j)} \quad (1)$$

$$20 \quad C_c(TE1, j) = C(TE1, j) * F(TE1, j) \quad (2)$$

21
22
23
24
25
26
27 90 Where, $F(TE1, j)$, $M(TE2, j)$, $C(TE1, j)$, and $C_c(TE1, j)$ are the correction factors at the “*j*th” TE1,
28
29 91 average marrow intensity at the “*j*th” TE2, average cortical bone intensity at the “*j*th” TE1, and
30
31 92 corrected image intensity at the “*j*th” TE1. To improve model fits in low signal to noise data,
32
33 93 images were corrected according to the methods of Miller and Joseph ⁽¹⁴⁾ and individually
34
35 94 modeled using a double exponential decay ⁽⁷⁾, with the following modifications:
36
37

$$38 \quad S(TE1, k) = ae^{\left(\frac{-TE1}{T2_B^*}\right)} + be^{\left(\frac{-TE1}{T2_F^*}\right)} \quad (3)$$

$$39 \quad \%B(k) = \frac{a}{(a + b)} 100 \quad (4)$$

$$40 \quad \%F(k) = 100 - \%B(k) \quad (5)$$

41
42
43
44
45
46
47
48
49 95 Where, TE1, a , $T2_B^*$, b , $T2_F^*$, and $S(TE1, k)$ are the variable TE as described above, intercept for
50
51 96 the bound fraction, $T2^*$ for the bound fraction, intercept for the free fraction, $T2^*$ for the free
52
53 97 fraction, and the noise-free signal decay for the “*k*th” subject. In order to compute the percent
54
55
56
57
58
59
60

1
2
3 98 bound (%B(k)) and free (%F(k)) water in the system for the “kth” subject, Eqns 4 and 5 were
4
5 99 employed.
6
7

8 100 *Statistics*

9
10
11 101 UTE-MRI data were evaluated using unpaired Students T-tests. Based on our previous work
12
13 102 showed improvement in hydration of raloxifene-treated bone, a one-tailed t-test was used. For
14
15 103 all statistical tests, *a priori* α -levels were set at 0.05.
16
17

18 104 **RESULTS**

19
20
21 105 Images acquired over the TE1 range from 0.05 to 1.1 ms resulted in high signal to noise ratios
22
23 106 which ranged from 3.89 ± 0.207 to 2.41 ± 0.093 , respectively (**Figure 1A-B**). Standardized
24
25 107 segmentation of UTE images resulted in uniform cortical ($170.0 \pm 10.5 \text{ mm}^3$) and marrow
26
27 108 ($62.2 \pm 3.79 \text{ mm}^3$) volume of interest, and when individually modeled yielded highly consistent
28
29 109 normalized signal as a function of TE1 (**Figure 1C**). The free and bound T2* time constants for
30
31 110 vehicle and raloxifene were 0.204 ± 0.027 , 5.02 ± 1.39 , 0.264 ± 0.021 , and 7.84 ± 1.59 ms,
32
33 111 respectively. UTE-MRI assessment of bound and free water was assessed in the cortical bone
34
35 112 of the proximal tibia (**Figure 2A&B**). Raloxifene treatment for 6 months led to significantly more
36
37 113 bound water (+14%) and significantly less free water (-20%) when compared to vehicle-treated
38
39 114 animals ($p=0.05$, $n=6/\text{grp}$).
40
41
42
43

44 115 **DISCUSSION**

45
46
47 116 Given the emerging interest in UTE-MRI as a tool to assess bone hydration ⁽⁷⁻¹⁰⁾ and the recent
48
49 117 evidence from our lab that raloxifene positively affects bone hydration ⁽⁶⁾ we undertook *in vivo*
50
51 118 measures of free/bound water in animals treated with raloxifene (or vehicle). Our results
52
53
54
55
56
57
58
59
60

1
2
3 119 provide exciting and novel data showing that raloxifene leads to higher bound water compared
4
5 120 to control animals and that this is detectable using *in vivo* UTE-MRI scanning.
6
7

8
9 121 Our analysis showed raloxifene treatment resulted in higher bound water – consistent
10
11 122 with our previous work ⁽⁶⁾. In addition, the rate constants from the UTE-MRI were consistent
12
13 123 with previous data in *ex vivo* bone samples ⁽⁷⁾. The mechanisms underlying raloxifene's positive
14
15 124 effects on bound water remain to be determined. Our previous work points to the increased
16
17 125 bound water at the collagen/mineral interface, effectively increasing the ability of the mineral
18
19 126 and collagen to dissipate energy and toughen the matrix. This effect occurs independent of
20
21 127 bone turnover and is cell-independent ⁽⁶⁾; although there are clearly cell-dependent effects of
22
23 128 raloxifene ⁽¹⁵⁾ and these could be contributing to changes in hydration.
24
25

26
27 129 The current study using UTE-MRI was only able to assess relative amounts of water
28
29 130 (bound/free). Thus, it's possible that changes in bound water were influenced by changes in
30
31 131 free water. Although we were not able to directly measure porosity, a major determinant of free
32
33 132 water, in these animals we have previously documented the intracortical turnover rate of tibia in
34
35 133 this age dog is 1-2% per year ^(16,17). Suppression of intracortical remodeling, as would be
36
37 134 expected with raloxifene, would therefore produce minimal changes in porosity, especially over
38
39 135 6 months (the remodeling cycle in a dog is ~ 3 months long ⁽¹⁸⁾). Based on this, it is unlikely free
40
41 136 water changes would account for the entire difference between groups quantified in the current
42
43 137 work. Future work should employ standards that allow absolute volumes of free/bound water
44
45 138 using UTE-MRI and/or should confirm these *in vivo* findings with *ex vivo* analyses by NMR.
46
47
48

49 139 These novel data show for the first time that drug-induced modulation of bone water can
50
51 140 be detected *in vivo* using UTE-MRI. Alterations in water, both increases and decreases, have
52
53 141 been shown to be associated with biomechanical properties ^(6,19). Having the ability to quantify
54
55
56
57
58
59
60

1
2
3 142 changes in hydration non-invasively will allow more detailed assessment to track not only how
4
5 143 raloxifene is altering bone properties, by how other interventions affect bone hydration, both in
6
7 144 preclinical and clinical studies.
8
9

10 145

11
12
13 146

14
15
16
17 147 **Acknowledgements.**

18
19
20 148 Funding for this study was provided by NIH (AR 62002 and a BIRT supplement). Raloxifene
21
22 149 was provided by through an MTA with Eli Lilly.
23
24

25 150
26
27
28
29
30
31
32
33
34
35
36
37
38
39
40
41
42
43
44
45
46
47
48
49
50
51
52
53
54
55
56
57
58
59
60

1
2
3 151 **Figure Legends**
4
5

6 152 **Figure 1.** Images of tibia cross-section (arrow), surrounded by muscle, from the transverse
7
8 153 UTE-MRI at a TE1 of 0.05 (A) and 1.1 ms (B) illustrating the image quality over the range of
9
10 154 TE1 studied. Panel C provides a chart of average normalized signal for with model fits (solid
11
12 155 lines) for VEH (n=6, solid) RAL (n=6, open). Data presented as means \pm standard error of the
13
14 156 mean.
15
16

17
18 157
19
20
21 158 **Figure 2.** Raloxifene leads to higher bound water (A) and lower free water (B) in the cortical
22
23 159 bone following 6 months of treatment. *In vivo* assessment of hydration was done using UTE-
24
25 160 MRI. n= 6 animals per treatment group. Data presented as means \pm standard error of the
26
27 161 mean. * p = 0.05 between groups using a one-tailed t-test as described in the statistics section.
28
29
30
31 162
32
33
34
35
36
37
38
39
40
41
42
43
44
45
46
47
48
49
50
51
52
53
54
55
56
57
58
59
60

163 **References**

- 1
2
3
4
5
6 164 1. Ettinger B, Black DM, Mitlak BH, Knickerbocker RK, Nickelsen T, Genant HK,
7 165 Christiansen C, Delmas PD, Zanchetta JR, Stakkestad J, Glüer CC, Krueger K, Cohen
8 166 FJ, Eckert S, Ensrud KE, Avioli LV, Lips P, Cummings SR. Reduction of vertebral fracture
9 167 risk in postmenopausal women with osteoporosis treated with raloxifene: results from a 3-
10 168 year randomized clinical trial. Multiple Outcomes of Raloxifene Evaluation (MORE)
11 169 Investigators. *JAMA*. 1999 Aug 18;282(7):637–45.
- 12
13
14 170 2. Riggs B, Melton L III. Bone turnover matters: the raloxifene treatment paradox of dramatic
15 171 decreases in vertebral fractures without commensurate increases in bone density. *J Bone*
16 172 *Miner Res*. 2002;17(1):11–4.
- 17
18 173 3. Sarkar S, Mitlak BH, Wong M, Stock JL, Black DM, Harper KD. Relationships between
19 174 bone mineral density and incident vertebral fracture risk with raloxifene therapy. *J Bone*
20 175 *Miner Res*. 2002 Jan;17(1):1–10.
- 21
22 176 4. Allen MR, Iwata K, Sato M, Burr DB. Raloxifene enhances vertebral mechanical
23 177 properties independent of bone density. *Bone*. 2006;39(5):1130–5.
- 24
25 178 5. Allen M, Hogan H, Hobbs W, Koivuniemi A, Koivuniemi M, Burr D. Raloxifene enhances
26 179 material-level mechanical properties of femoral cortical and trabecular bone.
27 180 *Endocrinology*. 2007;148(8):3908–13.
- 28
29
30 181 6. Gallant MA, Brown DM, Hammond M, Wallace JM, Du J, Deymier-Black AC, Almer JD,
31 182 Stock SR, Allen MR, Burr DB. Bone cell-independent benefits of raloxifene on the
32 183 skeleton: A novel mechanism for improving bone material properties. *Bone*. Elsevier Inc;
33 184 2014 Apr 1;61(C):191–200.
- 34
35 185 7. Diaz E, Chung CB, Bae WC, Statum S, Znamirowski R, Bydder GM, Du J. Ultrashort
36 186 echo time spectroscopic imaging (UTESI): an efficient method for quantifying bound and
37 187 free water. *NMR Biomed*. 2011 Jul 15;25(1):161–8.
- 38
39 188 8. Biswas R, Bae W, Diaz E, Masuda K, Chung CB, Bydder GM, Du J. Ultrashort echo time
40 189 (UTE) imaging with bi-component analysis: Bound and free water evaluation of bovine
41 190 cortical bone subject to sequential drying. *Bone*. Elsevier Inc; 2012 Mar 1;50(3):749–55.
- 42
43 191 9. Du J, Hermida JC, Diaz E, Corbeil J. Assessment of cortical bone with clinical and
44 192 ultrashort echo time sequences. *Magnetic Resonance Medicine*. 2013;70:697–704.
- 45
46
47 193 10. Techawiboonwong A, Song HK, Leonard MB, Wehrli FW. Cortical Bone Water: In Vivo
48 194 Quantification with Ultrashort Echo-Time MR Imaging. *Radiology*. 2008 Aug
49 195 18;248(3):824–33.
- 50
51 196 11. Aref M, Gallant MA, Organ JM, Wallace JM, Newman CL, Burr DB, Brown DM, Allen MR.
52 197 In vivo reference point indentation reveals positive effects of raloxifene on mechanical
53 198 properties following 6 months of treatment in skeletally mature beagle dogs. *Bone*. 2013
54 199 Oct;56(2):449–53.
- 55
56
57
58
59
60

- 1
2
3 200 12. Allen M, Iwata K, Phipps R, Burr D. Alterations in canine vertebral bone turnover,
4 201 microdamage accumulation, and biomechanical properties following 1-year treatment
5 202 with clinical treatment doses of risedronate or alendronate. *Bone*. 2006;39(4):872–9.
- 7 203 13. Li S, Chang EY, Bae WC, Chung CB, Hua Y, Zhou Y, Du J. The effect of excitation and
8 204 preparation pulses on nonslice selective 2D UTE bicomponent analysis of bound and free
9 205 water in cortical bone at 3T. *Med Phys*. 2014 Feb;41(2):022306.
- 11 206 14. Miller AJ, Joseph PM. The use of power images to perform quantitative analysis on low
12 207 SNR MR images. *Magn Reson Imaging*. 1993;11(7):1051–6.
- 14 208 15. Bryant HU, Glasebrook AL, Yang NN. A pharmacological review of raloxifene. *J Bone*
15 209 *Miner Metab*. 1996;14:1–9.
- 17 210 16. Allen M, Kubek D, Burr D. Cancer treatment dosing regimens of zoledronic acid result in
18 211 near-complete suppression of mandible intracortical bone remodeling in beagle dogs. *J*
19 212 *Bone Miner Res*. 2010;25(1):98–105.
- 21 213 17. Allen MR, Kubek DJ, Burr DB, Ruggiero SL, Chu T-MG. Compromised osseous healing
22 214 of dental extraction sites in zoledronic acid-treated dogs. *Osteoporos Int*. 2011
23 215 Feb;22(2):693–702.
- 25 216 18. Boyce RW, Paddock CL, Gleason JR, Sletsema WK, Eriksen EF. The effects of
26 217 risedronate on canine cancellous bone remodeling: Three-dimensional kinetic
27 218 reconstruction of the remodeling site. *J Bone Miner Res*. 2009;10(2):211–21.
- 29 219 19. Bae WC, Chen PC, Chung CB, Masuda K, D'Lima D, Du J. Quantitative ultrashort echo
30 220 time (UTE) MRI of human cortical bone: correlation with porosity and biomechanical
31 221 properties. *J Bone Miner Res*. 2012 Apr;27(4):848–57.

222

1
2
3
4
5
6
7
8
9
10
11
12
13
14
15
16
17
18
19
20
21
22
23
24
25
26
27
28
29
30
31
32
33
34
35
36
37
38
39
40
41
42
43

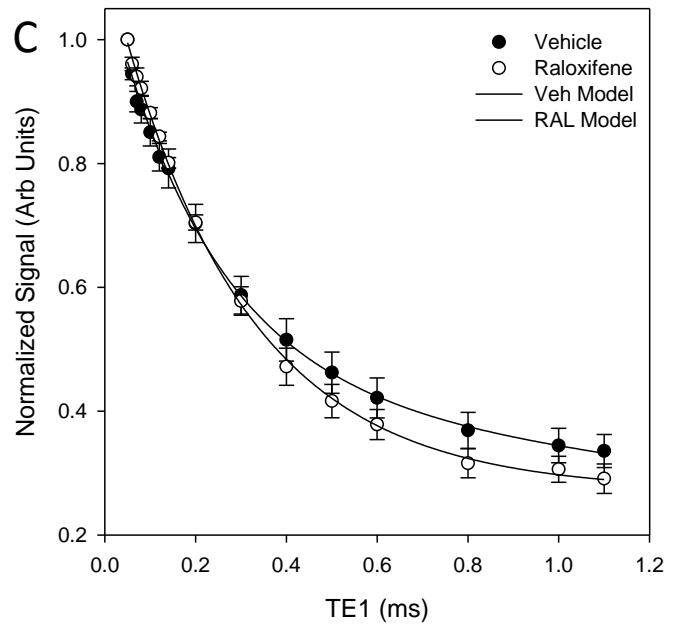


Figure 1

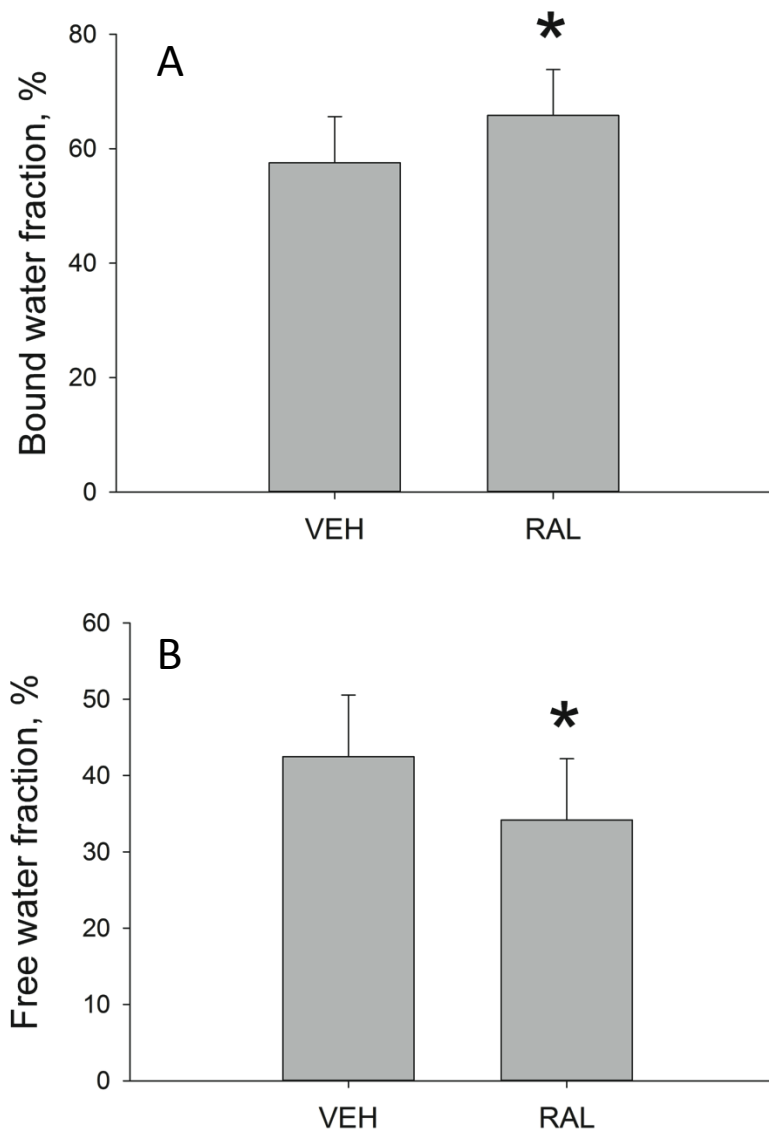


Figure 2

1
2
3
4
5
6
7
8
9
10
11
12
13
14
15
16
17
18
19
20
21
22
23
24
25
26
27
28
29
30
31
32
33
34
35
36
37
38
39
40
41
42
43